Structure Design and Indirect Adaptive General Predictive Temperature Control of a Class of Passive HVAC

TAWEGOUM Rousseau
Unité Propre EPHor (Environnement Physique de la plante Horticole)
Institut National d'Horticulture
2, rue Le Nôtre 49045 ANGERS
FRANCE
rousseau.tawegoum@inh.fr

Abstract: **-** This study focuses firstly on the numerical investigation of an air conditioning unit prototype developed to guarantee a microclimate with controlled temperature and relative humidity set points for crop growth chambers. Numerical techniques based on Computational Fluid Dynamics (CFD) were implemented to estimate component size and to analyze the flow characteristics of the mixed air produced by the device. Simulations disclose a non-linear relationship between the air flow rate and the aperture opening, and also show that the mixing zone was not perfect but could be improved by the addition of baffles. The promising results obtained from CFD were used to improve the automation of the device for potential application in closed greenhouses. Secondly, the indirect adaptive generalized predictive control strategy (IAGPC) with a decentralized architecture was used to control the temperature of the air conditioning unit. As the process involves time-varying, the use of a recursive estimation approach with a fixed forget factor was adopted to estimate in real time the system parameters, and to adapt simultaneously the GPC controller parameters. In order to achieve a local and global efficient performance, the proposed decentralized IAGPC architecture was applied to two principal subsystems, which compose the global unit. A significant real time experimental improvement in the system performance is observed on temperature control for a wide range of operating points.

Key-Words: numerical simulation, air flow distribution, time varying parameters, decentralized control, adaptive control.

1 Introduction

The energy consumption by the heating, by ventilation and by air conditioning equipment in the industrial buildings, constitutes 50% of the world energy consumption [1]. Among these buildings, one distinguishes horticultural greenhouses, which present an important branch of the agriculture sector [2], [3]. The optimal management of the greenhouse or growth chamber microclimate (temperature, moisture) is a dominating factor, on the one hand to deal with the market quantitative and qualitative requirements [4], [5] and on the other hand to ensure a possible better economic profitability for the farmers.

In general, air conditioning units used in crop growth chambers are often made up of elements of heating and cooling systems with a compression cycle [6], [7]. In addition to the energy cost and the high expenses of maintenance of this type of systems, they present also an ecological problem because of the pollutant emissions due to the used refrigerating gases.

The main cooling technologies routinely used in greenhouses are ventilation, evaporative cooling, and composite systems. A simple way to reduce the difference between inside and outside air temperature is to improve ventilation. Natural ventilation uses very little external energy, but whether it is natural or forced, ventilation is of limited efficiency and not satisfactory on sunny days.

Evaporative cooling using fan-pads [8] or fog/mist [9] inside greenhouse and roof cooling systems [10] represents an efficient means of greenhouse cooling that can lower the inside air temperature significantly below the ambient air, but the range of relative humidity variation remains limited. Fan-pads work on negative pressure, so that very often outside hot air mixes with the inside cool air through infiltration, which reduces the efficiency of the system quite significantly. Mist or fog systems can provide more uniform temperature distribution than fan-pad systems, in addition to ensuring uniform high humidity levels. One of the drawbacks of fog mist is that the compressor consumes large amounts of energy, which

increases the cost of operating the system. This method also uses expensive foggers or nozzles, which often shocked due to insoluble and soluble salt present in the water, thereby reducing the working efficiency of the system.

Apart from these systems, two primary composite systems, such as earth-to-air heat exchangers (EAHES) and aquifer coupled cavity flow heat exchangers (ACCFHES), can be used for heating as well as cooling greenhouses. The EAHES uses the earth potential for heating and the ground potential of the earth for cooling the greenhouses in summer conditions due to its constant year round temperature. In this case, hot greenhouse air is circulated through the buried pipe (2-4m depth) for dissipation of heat to the underground soil. The aquifer coupled cavity flow heat exchanger system [11] uses deep underground aquifer water from an irrigation tube well at the ground surface at nearly constant temperature. The major disadvantage of using EAHES is the cost of digging and laying the pipes. Deterioration of the pipes under soil pressure also makes this system less reliable for projects of long duration.

For those reasons, we have investigated an alternative system, which is passive and does not use the more typical compression device or absorption-refrigeration cycle. The unit can also be helpful in investigation of relative humidity changes and the morphological responses of the plant (growth stoppage, floral transformation, delayed blossom-time, dormancy, etc...). At this design stage, the unit shape and the temperature control are our area of interest.

This paper proceeds as follows. The first part presents the system requirements. The second part focuses the numerical studies conducted based on partial differential equations models with the aim to better understand the mixing process and to forecast the device behaviour for a set of operating conditions. The last part proposes the synthesis of indirect adaptive generalized predictive control law based on differential equations models, with a decentralized architecture in order to manage the air conditioning temperature intended to produce a specific climate in growth chambers.

2 Problem Formulation

The micro-climate needed must be produced by a passive air-conditioning system that is without a freezing unit and compressor, or refrigeration cycle, and without pollutant emissions [12]. The specificity of this system is to produce a variable microclimate with variable temperatures and relative humidity set points. Since temperature and relative humidity are highly coupled, one way to achieve these objectives is to delink the control of the temperature from the relative humidity control.
The air-conditioning cycle is presented graphically below

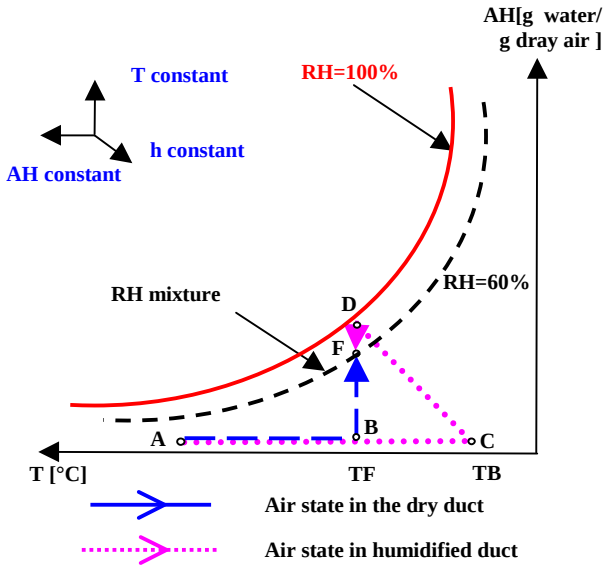

Fig. 1 : Thermodynamic cycle of the unit

Figure 1 shows the different thermodynamic phases of the air-conditioning cycle and the region corresponding to our zone of interest. The system depends on the mixing two air flows, each with a different humidity level. The air intake can be from inside greenhouse (point B) or outside greenhouse (point A). Regardless of the source of the air supply, the characteristics of the air are clearly defined.
The characteristics of the air at point F are also known because the final temperature T_F has to track the temperature of the second growth chamber, and the moisture RH_F is prescribed by the user. As the air heating operates at a constant absolute humidity, point B can be easily found by knowing the value T_F.
The computation of the characteristics of the air at point C is more complex. These characteristics can be deduced from point D, at which the temperature equals T_F. In D, air must be practically saturated. As cooling humidification (from C to D) operates at constant enthalpy, point C can be calculated by knowing the characteristics of points D and A.
Based on the enthalpy values of points A, B and C, the energy needed for heating can be computed.

The air flow rate required to obtain the relative humidity set point is computed using the relative evolution of the line 'D-B'. Considering the values of q_i, the final expressions of the absolute humidity (absolute moisture content) and of the temperature are given by:

$$AH_F = \frac{q_1.AH_B + q_2 AH_D}{q_1 + q_2} \quad (1)$$

$$T_F = \frac{q_1(\alpha+\beta AH_B)T_B + q_2(\alpha+\beta AH_D)T_D}{q_1(\alpha+\beta AH_B)+q_2(\alpha+\beta AH_D)} \quad (2)$$

with $\alpha = 0.24$, $\beta = 0.46$ and q_i is the air-flow mass proportional to the aperture position. Knowing both AH_F and T_F gives a unique value of RH_F [9].

3 Numerical simulation and air-conditioning design

3.1 Conditioning unit distributed model

3.1.1 Turbulence model

CFD simulations were carried out with the commercially available package Fluent 6.1. The method is based on the solution of the 2D-3D convection-diffusion equation which, for incompressible fluids and under steady state conditions, may be written as:

$$\frac{\partial(U\phi)}{\partial x} + \frac{\partial(V\phi)}{\partial y} + \frac{\partial(W\phi)}{\partial z} = \Gamma\Delta\phi + S_\phi \quad (3)$$

where ϕ represents the concentration of the non-dimensional transported quantity, namely momentum, mass and energy; U, V and W are the components of the velocity vector; Γ is the diffusion coefficient and S_ϕ is the source term.

The equations are Reynolds-averaged Navier-Stokes and the solution variables in the instantaneous Navier-Stokes equation are decomposed into mean and fluctuating components. The classical turbulence k-ε closure model is chosen because of its good ability to describe fully developed turbulent flows. The above mentioned equations are discretized on a triangular-cell grid. The grid is refined close to orifices where strong velocity gradients may occur.

3.1.2 Energy equation

In order to take into account heat transfer between heater an air, the energy equation is used in the following form:

$$\frac{\partial(\rho E)}{\partial t} + \nabla(\vec{v}(\rho E + p)) = \nabla(k_{eff}\nabla T - \sum_j h_j \vec{J}_j) + S_h \quad (4)$$

where k_{eff} is the effective conductivity, $\vec{J}_j$ is the diffusion flux of species j. The first two terms of the right-hand side of the above equation represent energy transfer due to the conduction, species diffusion. S_h includes volumetric heat sources.

$$E = h - \frac{p}{\rho} + \frac{v^2}{2} \quad (5)$$

where the sensible enthalpy h is defined for incompressible flows as:

$$h = \sum_j Y_j h_j + \frac{p}{\rho} \quad (6)$$

Y_j is the mass fraction of species j and

$$h_j = \int_{T_{ref}}^{T} c_{p,j} dT \quad (7)$$

where T_{ref} is 298 K.

3.1.2 Porous media.

3.1.2.1 Air-water heat and mass transfer in pads

Evaporative cooling involves no change in the heat content of the air/water vapour mixture. Rather, as water evaporates it takes away heat from the air thus reducing its temperature. This technology is based on the conversion of sensible heat into latent heat of evaporated water. During theses process, the enthalpy of the air remains the same. As shown on figure 1, air travelling from C to D must be saturated at D.

In order to estimate the length of the pads ensuring air saturation, simulation based on heat and mass transfers [13] between air and water through the pads were conducted, with the following assumption:

- the weak thickness of the pads make that, their contribution to heat transfer is neglected.
- the enthalpy of evaporated water is lower compared to other energies at work.

Pads are seen as a counterflow direct contact liquid gas exchanger.

The finite difference method with Cartesian co-ordinates were used to discretize conservation laws. Let us consider a grid element of step size $(\Delta x, \Delta z)$, the enthalpy variation in a mesh is of the form:

$$ha_{a,o} - ha_{a,i} = \varepsilon \times (h_{sat,i} - h_{a,i}) \quad (8)$$

with ε the exchanger efficiency defined as

$$\varepsilon_{x,z} = \frac{1 - e^{-\frac{K_D \Sigma}{G}.(\Delta x + m\Delta z)}}{1+m} \quad (9)$$

m is a local coefficient of the mesh given by the following expression:

$$m = \frac{(Csat)_{x,z}.G.\Delta z}{C_{p,e}.L.\Delta x} \quad (10)$$

where $(Csat)_{x,z} = \left(\frac{dh_{sat}}{dT_w}\right)_{x,z}$ is constant in a mesh

Subscripts a, w, i, o and sat stand respectively for air, water, input, output and saturation.
Σ is the volumic area, $C_{p,e}$ the mass specific heat, G the gaz area flow rate, h the enthalpy, Kc the convective heat coefficient, K_D the mass transfer coefficient, L the liquid area flow rate, T the temperature and AH the absolute humidity.

The air absolute humidity variation in the mesh is:

$$AH_{a,o} - AH_{a,i} = (AH_{sat,i} - AH_{a,i}) \quad (11)$$

Then the temperature of the air leaving a mesh takes the form

$$T_{a,o} = T_{a,i} + \varepsilon \times (T_{w,i} - T_{a,i}) \quad (12)$$

and the temperature of the water exiting a mesh is

$$T_{w,o} = T_{w,i} - \frac{G.\Delta z}{L.\Delta x.C_{p,e}}.(h_{a,o} - h_{a,i}) \quad (13)$$

3.1.2.2 Pressure drop

The corrugated pads create a sink of momentum due to friction forces (drag forces) of airflow through the pads. The pads are considered as macro-porous media in which the Darcy-Forchheimer model is assumed valid [14], [15]:

$$-\frac{\Delta p}{L} = \left(\frac{\mu}{\alpha} + \frac{C_2}{2}\|v\|\right) v_i \quad (14)$$

where L is the thickness of the pads, α is a coefficient independent of the nature of the fluid but depending on the geometry of the medium. It has the dimension of a squared length and is called the specific permeability of the medium. C_2 is a dimensionless form-drag constant dependent on the nature of the porous medium and is called inertial factor, ε is the void fraction, d is the equivalent diameter of the pores, μ is the air dynamic viscosity, ρ is the air density, v_i are the velocity components. The first term on the right-hand side (Darcy's term) accounts for the microscopic viscous drag while the second term accounts for the form drag which is due to inertial effects (direction changes) inside the pores and to turbulent dissipation.

3.1.3 Virtual tracer gas technique.

The species transport model without reaction was activated to solve the mixing problem. The governing equation was written as:

$$\frac{\partial}{\partial t}(\rho C) + \nabla(\rho \vec{v} C) = -\nabla \vec{J} + S \quad (15)$$

with C, the concentration of the transported quantity, S, the mass source term of the considered species, $\vec{J}$, the diffusion flux. S was set to zero in the air mixing computation, and equal to the water source mass in the pads during humidification investigation. The diffusion flux $\vec{J}$ was expressed as follows:

$$\begin{aligned} \vec{J} &= -(\rho D_m + \rho D_t)\nabla C - D_T \frac{\nabla T}{T} \\ &= -(\rho D_m + \frac{\mu_t}{S_{ct}})\nabla C - D_T \frac{\nabla T}{T} \end{aligned} \quad (16)$$

with D_m, the mass diffusion coefficient, D_t, the turbulent diffusivity, μ_t, the turbulent viscosity, S_{ct}, the turbulent Schmidt number, D_T, the thermal diffusion coefficient and T, the temperature.
Knowing the inlet air velocity, a converged steady-state solution of the k-ε model is first obtained for the velocity and pressure field. Unsteady state calculations were then conducted for the tracer gas: at time t=0, all the cells in the saturated flow of the conditioning unit had a water mass fraction set to unity whereas the cells of the unsaturated duct had a zero water mass fraction (dry air). Then, the transport equation of the virtual gas tracer was solved independently, using the previously calculated velocity field. The thermal effect was disabled when using this transport equation.

3.1.4 Boundary Conditions

The boundary conditions considered at the inlet circular section, of diameter 0,02m², were homogeneous velocities of 1,5 m s^{-1}, 2 m s^{-1}, 4 m s^{-1} and 8 m s^{-1} respectively, which were assumed to be normal to the section. The outlet section varied from 0,003 to 0,015 m², and the boundary conditions were outflow with zero output gradients. A classical wall function was imposed at the solid boundaries (wall). These were later considered as adiabatic. The turbulence parameters were determined specifying the turbulence length scale and the hydraulic diameter [16]. The CFD package Fluent and Matlab were used to conduct

simulations. CDF package is nowadays an efficient tool for numerical simulation in various domains [17], [18].

3.2 Simulation result and process design

Fig. 2 shows the contours of the velocity magnitude when pads are not included. One can observe the preference way of the air flow and its heterogeneous distribution. The next simulation (fig.3) demonstrates that the use of pads contributes to a reduction of the vortex and an improvement in homogeneity of the air distribution in the duct (fig 4). Figure 5 makes appear that whatever the relative humidity of the intake air, three pads of 10 cm length ensure the saturation. The influence of the pads is significant, the main advantage being the accurate saturation of air leaving the pads. One can also observe (fig 5) that, the heat transfer between air and water in the pads indicates that depending of the air intake and the water characteristics they temperature converge when air leaves the pads

Figure 7 shows the behaviour of the mixing zone in the original device. There is no migration of species in the mixing zone. The molecular diffusion seems to be much smaller than the turbulent diffusion. When baffles were added downstream the unit, the mixing was much better as shown in Figure 3.

Figure 8 shows the temperature distribution for a heating power of 6kW. Air temperature decreases through the pads, simulated using the developed UDF was in agreement with the predictions of air humid diagram. In other to obtain air output relative humidity, in the saturated duct equals 100% for CFD simulations, a maximum value of water transfer to air in the pads was imposed. More results can be found in [16].

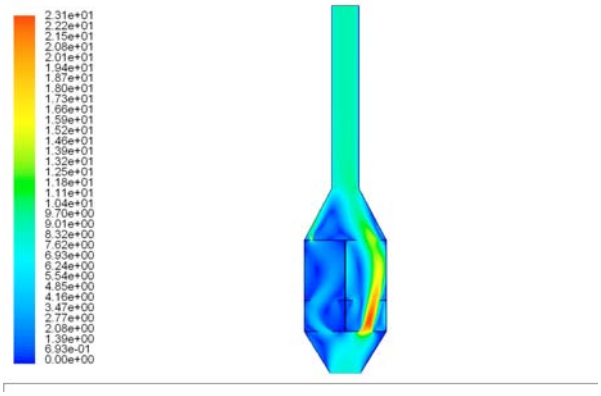

Fig. 2. Contours of velocity magnitudes ms^{-1} (inlet velocity 8 ms^{-1}, opening 10%-90%)

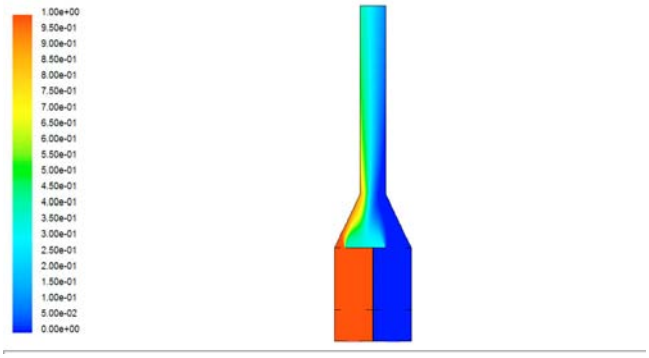

Fig. 3. Contours of mass fraction of air, inlet velocity 4 m s^{-1}, opening 20%-80%.

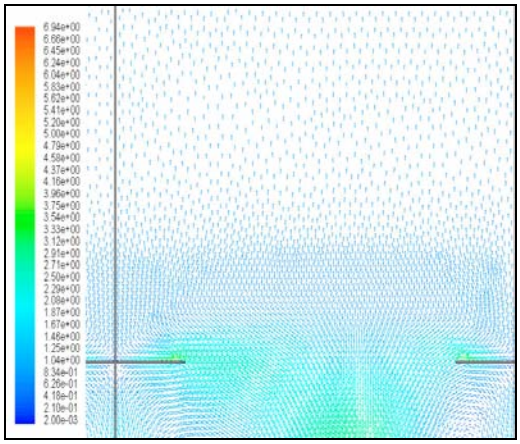

Fig. 4. Velocity field (ms^{-1}) in front and in the pads

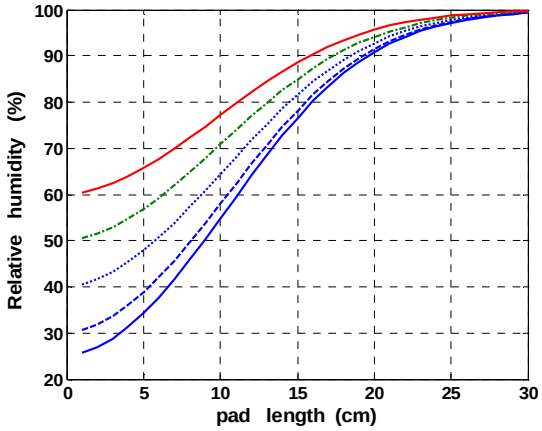

Fig. 5. Relative humidity behaviour within the pads

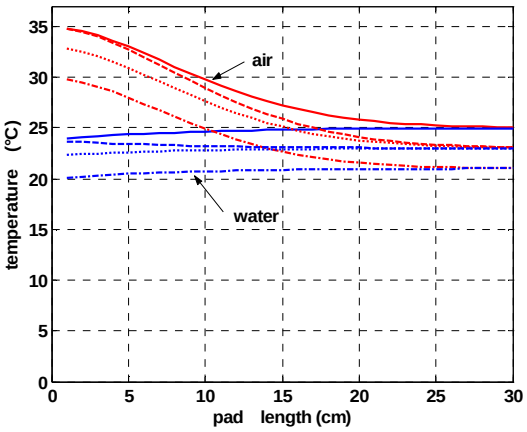

Fig. 6. Air and water behaviour within the pads

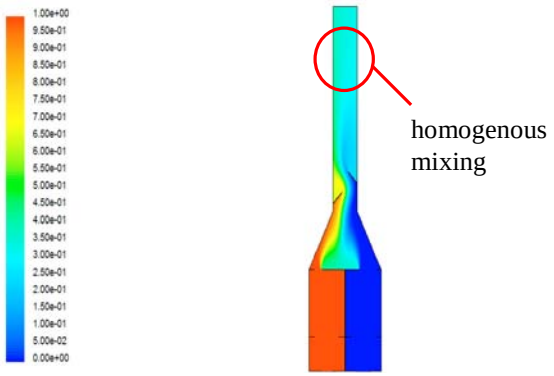

Fig. 7. Device with baffles : Contours of mass fraction of air, inlet velocity 4 m s^{-1}, opening 20%-80%.

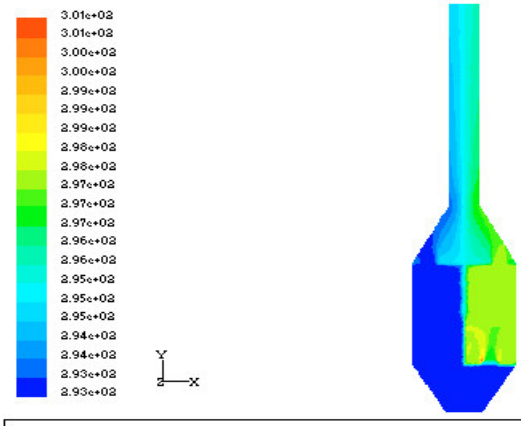

Fig. 8. Temperature field, heat source 6kW, inlet velocity 4m/s, opening 50%-50%.

The final form of the air conditioning device is presented on figure 9.

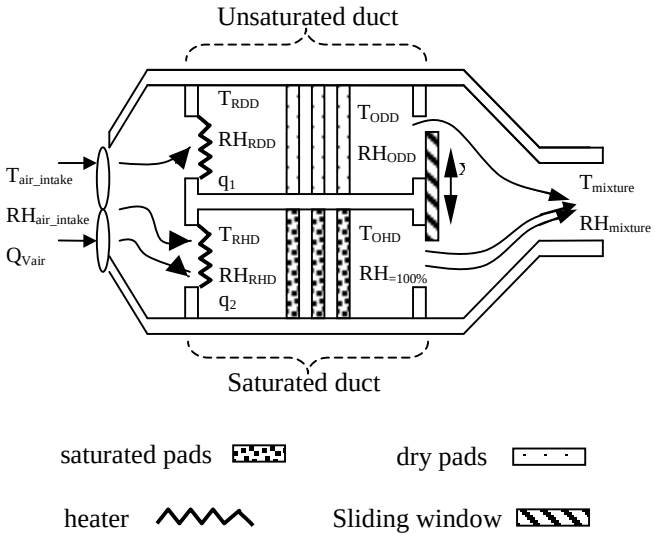

Fig. 9 Cross section view of the air-conditioning unit

The unit is composed of two flows: a non-saturated flow (or dry duct) and a saturated flow (or humidified duct) [16]. As shown in “Figure 1”, in the saturated air flow, fresh air is saturated in humidity after being heated by a coil resistor. Saturation operates at constant [13]. The saturation unit consists of a closed system, including a pump, a water tank and cross-corrugated cellulosic pads of the type used in cooling. The suction pump carries water from the tank to the top of the pads. Once a steady state of saturation is reached, the pads contain a constant mass of water with a given water output and a given temperature. In the unsaturated air flow, fresh air is only heated by another resistor coil. Dry pads are included to provide pressure drop balance. The low speed of the air and of the water through the pads reduces the difference of pressure drop between the two streams.

The proportional mixing of the two air flows is carried out by an aperture operated by a DC motor. Assuming that the two air flows are well mixed, a local climate can be easily produced in the growth chamber. A complete physical model of the device is presented in [17]. As the system is nonlinear and time varying parameters, an adaptive predictive approach was used to control the temperature.

4 Indirect Adaptive GPC temperature control

4.1- Indirect Adaptive GPC theory

Considering the complexity of the air conditioning model, the decentralized control architecture was selected to carry out the thermodynamic objective described by the psychometric diagram (Figure 1).
The aim of the thermodynamic strategy is to guarantee the same temperature set point for each duct. Since the steady state temperatures in the dry and humidified ducts are obtained, the set point temperature will be guaranteed for an air mixture as shown in fig. 1. In order to validate the feasibility of this thermodynamic strategy by the air conditioning unit, we are first focused on the control of different temperatures of each sub-system in spite of air intake variation and variable operating conditions Figure 6.
The predictive control algorithms based on generalized predictive control or even long range predictive control strategies have proved to be efficient, flexible and successful for industrial applications [18], [19], [20], [21], [22], [23], [24] [25], [26]. This strategy is associated with the recursive estimation algorithm in order to get better performance in both tracking and regulation problems.
The dynamic of conditioning unit can be described around an operating point by the following CARIMA equation:

$$A\left(q^{-1}\right)\Delta y(k) = B\left(q^{-1}\right)\Delta u(k-d) + C\left(q^{-1}\right)\varepsilon(k) \quad (17)$$

$y(k)$ is the system output, $u(k)$ the system input, $\varepsilon(k)$ the uncorrelated random sequence, $\Delta\left(q^{-1}\right)=1-q^{-1}$ the difference operator, $A\left(q^{-1}\right), B\left(q^{-1}\right), C\left(q^{-1}\right)$ are polynomials with n_a, n_b and n_c degree respectively.
The predictive output vector can be formulated as

$$\hat{y}(k+j) = G_j\left(q^{-1}\right)\Delta u(k+j-1) + \ell_j \quad (18)$$

where: $\ell_j = F_j\left(q^{-1}\right)y(k) + H_j\left(q^{-1}\right)\Delta u(k-1)$

Where: F_j, E_j, G_j, H_j are obtained by a recursive calculation of Diophantine equations proposed by [27], [28].
The controller design is based on the minimization of the following cost function:

$$J(k) = \sum_{j=N_1}^{N_2}\left(w(t+j) - \hat{y}(k+j)\right)^2 + \lambda\sum_{j=1}^{N_u}\left(\Delta u(k+j-1)\right)^2 \quad (19)$$

where: $\Delta u_j(k+j) = 0$, for $j \geq N_u$.
$w(k+j)$ are the set points values at time $k+j$, $\hat{y}(k+j)$ the output prediction at time $k+j$, N_1 the minimum prediction horizon, N_2 the maximum prediction horizon, N_u the control horizon, λ the control-weighting factor.
The control law is therefore given by

$$\Delta U_{opt} = \left[G^T G + \lambda\, I\right]^{-1} G^T (W - L) \quad (20)$$

With G is a $(N_2 - N_1 + 1)\times N_u$ matrix. Only the first control value is finally applied to the system according to the receding horizon strategy:

$$u_{opt}(k) = u_{opt}(k-1) + \bar{G}(W - L) \quad (21)$$

where, $\bar{G}$ is the first line of matrix $\left[G^T G + \lambda\, I\right]^{-1} G^T$.
The adaptive controller is obtained by simply invoking the certainty equivalence principle, which consists of replacing the process model parameters by their estimates when deriving the control law. To estimate the parameters of the model given by (17) and RLS parameter adaptation algorithm with fixed forgetting factors chosen to provide a better adaptation alterness was used [29].

4.2 Application to the process

The input-output temperature discrete model structure found was of the form:

$$\frac{T_{ODD}(k)}{U_{DD}(k)} = \frac{q^{-1}(b_{11}(k) + b_{12}(k)q^{-1})}{1 + a_{11}(k)q^{-1} + a_{12}(k)q^{-2} + a_{13}(k)q^{-3}} \quad (22)$$

for the dry duct, and

$$\frac{T_{OHD}(k)}{U_{HD}(k)} = \frac{q^{-1}(b_{21}(k) + b_{22}(k)q^{-1})}{1 + a_{21}(k)q^{-1} + a_{22}(k)q^{-2} + a_{23}(k)q^{-3}} \quad (23)$$

for the humid duct. T_{ODD}, T_{OHD}, are the output temperature of the dry duct and humid duct, while U_{DD} and U_{HD} are the voltage applied on the heater of the dry duct and the humid duct.

The recursive identification and GPC code developed with Matlab® software were connected to the industrial automation via a local area

network managed by interface developed with Delphi® software. A set of electronic units was used to apply heating voltage on the resistors or to control the DC motor and thus, the window opening rate. Measurements were carried out using Pt100 sensors for temperature and encoder sensors for window position. A sampling interval of Te=30 seconds was chosen to satisfy the predominant time constant, and data acquisition time about twelve hours. The operating point (aperture opening) values interval is $x \in [0\%,100\%]$. Figure 11 and 13 show the variations of the models parameters estimated in real time by the recursive algorithm. More results can be found in [30].

Generally speaking, control performance was good, as shown by the IAGPC for different set point values. The temperature ducts are closed to the set points in figures 10 and 12. The figures generally show an efficient disturbance rejection. These disturbances, caused by the intake air temperature, are eliminated by the integral action existing in the CARIMA basic model.

The control strategy robustness was also observed through temperature overshoot rejection. This type of disturbance is caused by the aperture commutation (operating point system variations) which in reality affects the air rate flow variation. At 700 th sampling time in figure 12, the overshoots presented by the humid duct air temperature response result from the abrupt aperture opening commutation, which introduces a parametric error estimation and, consequently, instantaneous closed loop instability between the 800 th and the 900 th sampling time. These can be explained by the non-persistence of the control signal in a steady state, causing the cross-correlation of the covariance matrix vectors, which leads to the estimator divergence.

In figure 14, the air temperature fluctuations do not appear between the 800 th and the 900 th sample time, such as in figure 12, because during this window of time, the humid duct was nearly closed ($10\% < x\% < 18\%$). As a result, its contribution to air mixing was reduced.

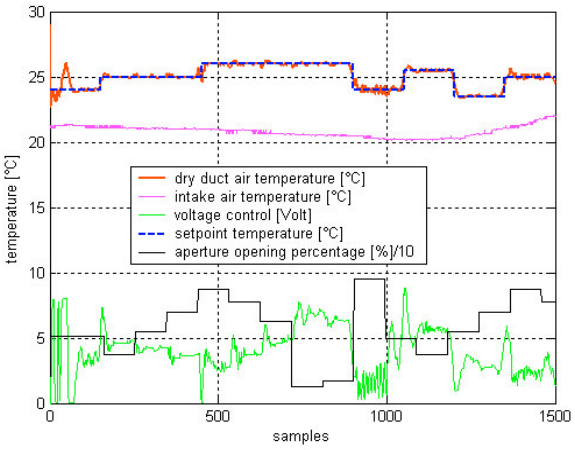

Fig. 10. IAGPC of the air dry duct temperature

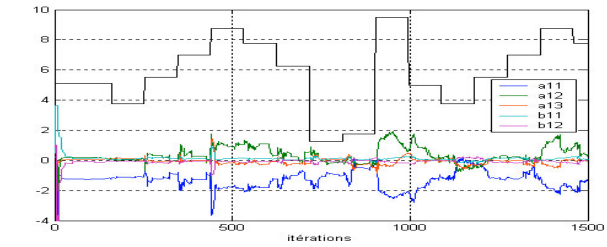

Fig.11. Dry duct model estimated parameters

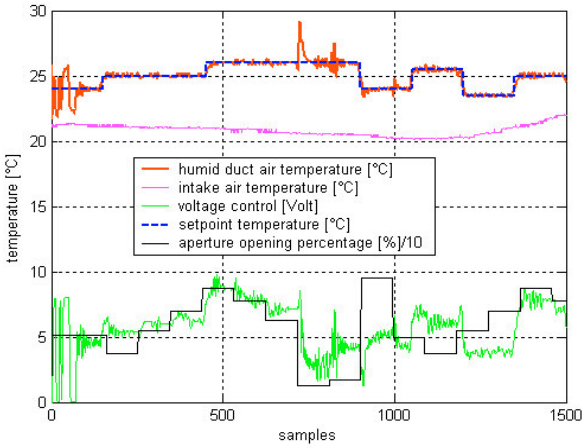

Fig.12. IAGPC of the air humid duct temperature

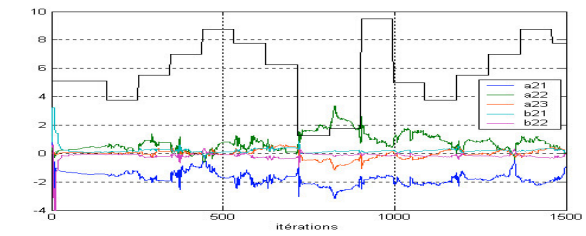

Fig.13. Humid duct model estimated parameters

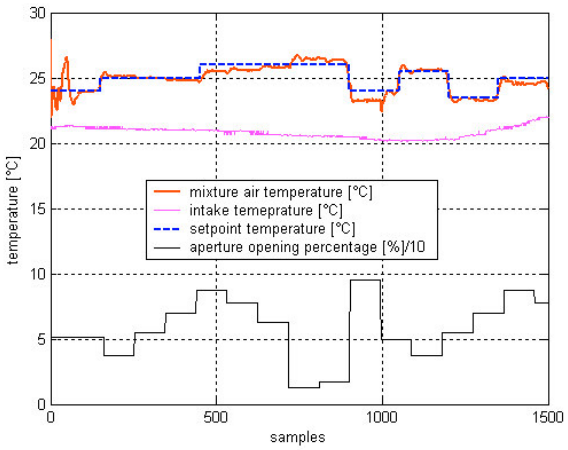

Fig.14. IAGPC of the air mixture temperature

To sum up, the air mixture temperature set points are guaranteed indirectly as consequence to the accuracy of the two temperatures at the upstream ducts Figure 14, with an accepted accuracy, showing the feasibility of the proposed humid air thermodynamic strategy.

5 Conclusion

A CFD software was developed to investigate airflow velocity, pressure and temperature fields, through an air-conditioning unit. Different configurations were tested and compared to experimental values. The results obtained describe and validate the nonlinear relationship between the airflow rate and the aperture opening, and the independence of this relationship to air inlet velocity values. Simulations also show that adding baffles downstream the unit enhanced the air mixing process. These results provide significant information on sensor locations in order to assess the real behaviour of the mixing. Ongoing studies are being conducted in order to understand the transient behaviour during set point modification and to improve the shape of the mixing zone using the shape optimization theory [31], [32].

Concerning the control aspect, the proposed IAGPC provides, an accepted robustness in spite of the parametric variation and the operating point changes. The relative humidity and the temperature control improvement will be brought by imposing the constraints on both outputs and input control. Taking into account a supervision stage on the local controllers is in study, to enhance the control performance.

References

[1] B.Arguello-Serrano, M. Vélez-Reye, « Non linear control of heating, ventilating, and air conditioning system with thermal load estimation », IEEE Transactions on Control Systems Technology, vol. 7, No. 1, January. 1999, pp. 56–63.

[2] P. Jones, J.W. Jones ., L.H. Allen, and J.W. Mishve « Dynamic computer control of closed environmental plant growth chambers », Design and Verification. Transaction of ASAE. (American Society of Agricultural Engineers), 1984, pp. 879-888.

[3] P.C. Young and M.J. Lees « Simplicity out of complexity in glasshouse climate modelling », in Proc. 2nd IFAC/ISHS Workshop on Mathematical an Control Application in agriculture and Horticulture, Silsoe, United kingdom, Acta Horticuturae N°406, 12-15 Sept 1994,pp.15-28.

[4] Albright, R.S Gates, K.G Aravantis and A.E. Drysdale, 2001. « Environment Control for Plants on Earth and Space » IEEE Control Systems Magazine, October 2001,pp. 28-47.

[5] J.B. Cunha and J.P.M. Oliveira, « Optimal management of greenhouse environments », EFITA Conference, Hungary, Dec 2003, pp. 559-564.

[6] J.J. Hanan «Greenhouse: advanced technology for protected horticulture», Chap 4, 1997, pp. 236-260.

[7] Hansen J.M. and Hogh Schimth K. A computer controlled chamber system design for greenhouse microclimatic modelling and control, in Proc. International symposium on plant production in closed ecosystems, ISHS, Acta Horticulturae 440: 1996, pp 105-110.

[12] Tawegoum R. , Teixeira R. and Chasseriaux G. 2006. Simulation of humidity control and greenhouse temperature tracking in a growth chamber using a passive air-conditioning unit. Control Engineering practice Journal. 14/8:853-861.

[9] Bailly M. Thermodynamique technique2.b, Machines thermiques et frigorifiques. Bordas. Paris-Montreal, 1971.

[14] Ergun S. Fluid flow through packed columns, Chem. Eng. Prog. 48,1952, pp 89-94.

[15] Fourar M and Lenormand R.. Inertial effects in two-phase flow through fractures, Oil & gas Science and technology, revue IFP (Institut Français du Petrole). vol 55, N°3 , 2000, pp 259-268.

[16] R. Tawegoum, P.E Bournet, J. Arnould, R.Riadi and G. Chassériaux. « Numerical investigation of an air conditioning unit to manage inside greenhouse air temperature and relative humidity », International Symposium on Greenhouse Cooling, Almeria-Spain, , April 2006, pp. 115-122.

[13] A. Chraibi, S. Makhlouf and A. Jaffrin « Refroidissement évaporatif de l'air des serres », Journal de Physique, n°III. Juillet 1995.

[17] R.Riadi, R.Tawegoum. A.Rachid, G.Chassériaux «Modeling and Identification of a Passive Air-Conditioning Unit using the Operating Dependent Parameters-Structure», CESA-2006: Computational Engineering in Systems Application, Beijing, Chine-4-6 Oct 2006, pp 1485-1491.

[18] J. Richalet, A. Rault, J. Testud and J. Papon

« Model predictive heuristic control: Applications to industrial processes », Automatica, , 1978, pp.413-428.

[19] T.G. Nybrant, « Modelling and adaptive control of concurrent flow driers » Computers and Electronics in Agriculture, 3, 1989, pp 243-253.

[20] A. Rafilamanana, A. Cabassud, M. V. LeLann and G. Casamatta, « Adaptive control of a multipurpose and flexible semi-batch pilot plant reactor», Comp. Chen. Eng. 16 (9), 1992, pp.837-848,.

[21] E. F. Camacho, C. Bordons, « Model predictive cntrol », Advanced textbooks in control and signal processing, Springer 2nd Edition.

[22] D. Dumur, P. Boucher, K.M Murphy, F. Déqué « On Predictive Controller Design for Comfort Control in Single Residential Housing »-,ECC'97, , juillet 1997, pp. 109-114.

[23] I.D. Landau, L. Dugard , « Commande adaptative aspects pratiques et théoriques » , J. Masson, Ed. Paris, 1986, pp. 1–81.

[24] N.M. Filataov, H. Unbedhauen, « Adaptive Dual Control: Theory and Applications », Springer, 2004.

[27] D.W. Clarke, C. Mohtadi, and P.S. Tuffs, « Generalized predictive control- part I. The basic algorithm », Automatica, 23(2), 1987, pp. 137-148.

[28] D.W. Clarke, C. Mohtadi, and P.S. Tuffs, « Generalized predictive control- part II. Extensions and interpretations », Automatica, 23(2) , 1987, pp. 149-160.

[29] L. Ljung, « System identification », Theory for the user, Prentice Hall, 1999.

[30] R.Riadi, R.Tawegoum. A.Rachid, G.Chassériaux, Denectralized temperature indirect adaptive predictive control of a passive air conditioning unit. Proceedinds of the 46th IEEE Conference on Decision and Control, New Orleans, LA, USA, Dec 12-14, 2007, pp 1808-1813

[8] Kittas, C.; Bartzanas, T. & Jaffarin, A. (2003). Temperature gradient in a partially shaded large greenhouse equiped with evaporative cooling pads, *Biosystems Engineering*, vol 85, N° 1, pp. 87-94

[9] Montero, J.J.; Anton, A.; Beil, C. & Franquet, A. (1994). Cooling of greenhouses with compressed air fogging nozzles, *Acta Horticulturae*, N°281, pp. 199-209.

[11] Sethi, V.P. & Sharma, S.K. (2007a). Experimental and economic study of a greenhouse thermal control system using aquifer water, *Energy Conversion and Management*, vol 48, N° 1, pp. 306-319.

[10] Willis, D.H. & Peet, M.M. (2000). Intermittent application of water to an externally mounted greenhouse shade cloth to modify cooling performance, *Transactions of ASAE*, vol 43, N° 5, pp. 1247-1252.

[25] I. I. Siller-alcalà, M. Abderrahim Fichouche, J. Jaimes-Ponce, and R. Alcantara-Ramirez, «Position predictive control for and induction motor», Proceedings of the 3rd WSEAS/IASME International Conference on Dynamical Systems and Control, Arcachon, France, October 13-15, 2007, pp.224-228.

[26] K. Belda and J. Böhm, « Range-space modication of predictive control for parallele robots », Proceedings of the 3rd WSEAS/IASME International Conference on Dynamical Systems and Control, Arcachon, France, October 13-15, 2007, pp. 235-240

[18] T.D. Karapantios, A.I. Balouktsis, D. Chassapis and M.D. Petala, «CFD model to estimate the effect of tilt and height on the natural air flow inside s solar chimney», Proceedings of the 7th International Conference on Electric power systems, High voltages, electric machines, Venice, Italy, Nov 21-23, 2007, pp. 53-58.

[17] R. Kamali, and A.R. Binesh «A CFD study of dimensional scaling effect on the combustion of hydrogen-air mixture in micro-scale chambers with same shape aspect ration », Proceedings of the 6th WSEAS International Conference on System science and simulation in engineering, Venice, Italy, Nov 21-23, 2007, pp. 231-236.

[31] J. Sokolowski ans J-P. Zolesio «Introduction to shape optimization», Spriger Verlag, 1992.

[32] G. Allaire, «Conception optimale de structures», Springer, 2007.